Supporting Information

Double-layered honeycomb architectures constructed via hierarchical self-assembly of hexagonal spin crossover cobalt(II) metallacycles

Ryohei Akiyoshi,[a] Keita Kuroiwa,[b] Mina Sakuragi,[b] Soichiro Yoshimoto,[c] Ryo Ohtani,[a] Masaaki Nakamura,[a] Leonard F. Lindoy,[d] and Shinya Hayami*[a,e]

[a] Department of Chemistry, Graduate School of Science and Technology, Kumamoto University, 2-39-1 Kurokami, Chuo-ku, Kumamoto 860-0855, Japan
[b] Department of Nanoscience Faculty of Engineering, Sojo University, 4-22-1 Ikeda, Nishi-ku, Kumamoto 860-0082, Japan
[c] Division of Materials Science and Chemistry, Faculty of Advanced Science and Technology, Kumamoto University, 2-39-1 Kurokami, Chuo-ku, Kumamoto 860-8555, Japan
[d] School of Chemistry, The University of Sydney, NSW 2006, Australia
[e] Institute of Pulsed Power Science (IPPS), Kumamoto University, 2-39-1 Kurokami, Chuo-ku, Kumamoto 860-8555, Japan

Email: hayami@kumamoto-u.ac.jp

Table of Contents

Experimental Section

General

All chemicals were purchased commercially and used without further purification. All organic syntheses were carried out under an Ar atmosphere. The synthesis of *R*-bisterpy, C_{12}-Glu$^-$Na$^+$ and [Co_6(*R*-bisterpy)$_6$](C_{12}-Glu)$_{12}$ were performed according to the previously reported literature procedure.[1,2]

Syntheses

Dialkyl-L-glutamate hydrochloride. *L*-Glutamic acid (5.00 g, 37.8 mmol), distilled 1-dodecanol (17.6 g, 10.0 mmol) and *p*-toluenesulfonic acid (8.07 g, 42.1 mmol) in dry toluene (100 mL) were heated under reflux for 5 h. The mixture was allowed to cool to room temperature and the toluene was removed under reduced pressure. The residue was dissolved in $CHCl_3$ and the resulting solution was washed with aqueous Na_2CO_3 (pH = 9) (50 mL × 3), distilled water (50 mL × 3), then dried over Na_2SO_4. It was then filtered and taken to dryness. The residue was dissolved in acetone (600 mL) and conc. HCl (6.7 mL, 120 mmol) was slowly added to the resulting solution. A colourless precipitate formed on standing the solution for 3 h in a refrigerator. The crude product was purified by recrystallizing from acetone to give the pure product as a colourless powder. Yield: 10.58 g (54%). ^{1}H NMR (500 MHz, $CDCl_3$): δ = 0.84 (t, 6H), 1.23 (m, 35H), 1.56 (dd, 4H), 2.01 (m, 2H), 4.00 (t, 2H), 4.13 (t, 2H), 8.76 (br, 2H, NH_2) ppm.

Sodium 4-(1,3-Bis-dodecyloxycarbonyl-propylcarbamoyl)-benzenesulfonate (C_{12}-Glu$^-$Na$^+$). Triethylamine (3.74 g, 37.0 mmol) in dry DMF (50 mL) was added to dialkyl-L-glutamate hydrochloride (5.44 g, 10.5 mmol) and *p*-sulfobenzoic acid as its potassium salt (2.52 g, 10.5 mmol) in dry DMF (50 mL) under cooling. To this mixture, 1*H*-benzotriazole-3-yl-oxy-tris(dimethyl)phosphorous hexafluorophosphate (BOP) (4.64 g, 10.5 mmol) in dry DMF (20 mL) was added slowly and the resulting mixture was stirred at room temperature for 12 h. After removing the DMF under reduced pressure, the residue was dissolved in $CHCl_3$, washed with saturated $NaHCO_3$ solution (50 mL × 3) and saturated NH_4Cl solution (50 mL × 3), dried over Na_2SO_4, filtered and evaporated. The crude product that remained was purified by recrystallizing from MeOH to give the product as a colourless powder. Yield: 4.13 g (57%). ^{1}H NMR (500 MHz, $CDCl_3$): δ = 0.84 (t, 6H), 1.22 (m, 38H), 1.54 (m, 4H), 2.01 (m, 2H), 4.06 (m, 4H), 4.42 (m, 1H), 7.66 (d, 2H), 7.81 (d, 2H), 8.75 (br, 1H) ppm.

3,5-Bis(terpyridinyl)benzene (bisterpy). 2-Acetylpyridine (13.3 g, 110 mmol) was added to

isophthalaldehyde (3.35 g, 25 mmol) in EtOH (300 mL). After stirring for 10 min, NaOH (4.39 g) in water (20 mL) was added. The mixture was stirred at room temperature for 12 h, then the solvent was removed under reduced pressure to afford a red oily residue, which was dried under reduced pressure for 24 h to generate a red powder. Ammonium acetate (52 g, excess) and glacial AcOH (300 mL) were added to a flask containing the red powder, and the resulting mixture was refluxed for 12 h to afford a dark brown solution. After removing the AcOH under reduced pressure, the dark oily residue that remained was dissolved in $CHCl_3$, washed with water (50 mL × 3), dried over $MgSO_4$, filtered and evaporated. The crude product was purified by column chromatography (neutral Al_2O_3) eluting with $CHCl_3$, followed by recrystallization from MeOH to give the product as a pale-yellow powder. Yield: 3.34 g (25%). ^{1}H NMR (500 MHz, $CDCl_3$): δ = 7.29 (d, 4H), 7.60 (t, 1H), 7.83 (t, 4H), 7.91 (d, 2H), 8.25 (s, 1H), 8.63 (d, 4H), 8.67 (d, 4H), 8.74 (s, 4H) ppm.

3,5-Bis(terpyridinyl)phenol (OH-bisterpy). *O*-Benzyl-bisterpy was synthesized using *O*-benzyl-isophthalaldehyde by the same procedure as employed for bisterpy. Pd/C (20 %, 100 mg) was added to a solution of *O*-Benzyl-bisterpy (900 mg) in THF (120 mL) and EtOH (20 mL). The resulting suspension was heated at 50℃ under a H_2 atmosphere for 24 h. The suspension was filtered through celite and evaporated under reduced pressure to give the product as a light-yellow powder Yield: 0.68 g (88%). ^{1}H NMR (500 MHz, DMSO-d_6): δ = 7.51 (s, 2H), 7.60 (t, 4H), 7.83 (s, 1H), 8.11 (t, 4H), 8.76 (d, 4H), 8.73 (m, 8H), 10.15 (br s, 1H).

3,5-Bis(terpyridinyl)benzene (*R*-bisterpy). A mixture of OH-Bisterpy (2.00 g, 3.6 mmol) and K_2CO_3 (5.00 g, 36 mmol) in MeCN (60 mL) was refluxed for 1 h, then 1-bromohexadecane (or 11-(4-bromobutyl)tricosane) (5.4 mmol) was added dropwise. The resulting mixture was refluxed for a further 24 h. After removing the solvent under reduced pressure, the residue was dissolved in $CHCl_3$. This was washed with 5 % K_2CO_3 in water (50 mL × 3), and the solution was then dried over $MgSO_4$, filtered, and evaporated. The crude product that remained was purified by column chromatography (silica gel, eluting with hexane and $CHCl_3$ in turn) to give the product as a white powder. Yield of C_{16}-bisterpy: 1.97 g (70%). Yield of $C_5C_{10}C_{12}$-bisterpy: 2.32 g (69%). ^{1}H NMR (500 MHz, $CDCl_3$): δ = 7.29 (d, 4H), 7.60 (t, 1H), 7.83 (t, 4H), 7.91 (d, 2H), 7.82 (t, 5H), 8.63 (d, 4H), 8.67 (d, 4H), 8.74 (s, 4H) ppm.

[Co_6(*R*-bisterpy)$_6$](BF$_4$)$_{12}$ (*R* = H (1), $OC_{16}H_{33}$ (2), $OC_{27}H_{55}$ (3)). *R*-Bisterpy (0.10 mmol) in $CHCl_3$ (20 mL) and $Co(BF_4)_2{\cdot}6H_2O$ (51 mg, 0.15 mmol) in MeOH (10 mL) were mixed and stirred for 3 h. In each case the product formed as an orange powder which was washed with MeOH and $CHCl_3$. Yield of **1**: 45 mg (9.8%). Yield of **2**: 63 mg (10.4%). Yield of **3**: 79 mg (11.2%). Anal.

$C_{216}H_{144}B_{12}Co_6F_{48}N_{36}$ + 3 CH_3OH (**1**): calcd. C 55.55, H 3.23, N 10.65; found. C 55.87, H 3.12, N 10.27. Anal. $C_{312}H_{336}B_{12}Co_6F_{48}N_{36}O_6$ + 4 CH_3OH (**2**): calcd. C 61.12, H 5.71, N 8.12; found. C 61.30, H 5.54, N 7.63. Anal. $C_{378}H_{468}B_{12}Co_6F_{48}N_{36}O_6$ (**3**): calcd. C 64.79, H 6.73, N 7.20; found. C 64.68, H 7.04, N 7.11. ESI-TOF-MS for **1** (positive mode): m/z = 1072.72 $[M(BF_4)_8]^{4+}$, 840.77 $[M(BF_4)_7]^{5+}$, 686.14 $[M(BF_4)_6]^{6+}$, 575.87 $[M(BF_4)_5]^{7+}$, 492.86 $[M(BF_4)_4]^{8+}$, 428.43 $[M(BF_4)_3]^{9+}$, 376.88 $[M(BF_4)_2]^{10+}$, 334.71 $[M(BF_4)_1]^{11+}$. ESI-TOF-MS for **2** (positive mode): m/z = 1939.78 $[M(BF_4)_9]^{3+}$, 1433.08 $[M(BF_4)_8]^{4+}$, 1129.07 $[M(BF_4)_7]^{5+}$, 926.39 $[M(BF_4)_6]^{6+}$, 781.62 $[M(BF_4)_5]^{7+}$, 673.04 $[M(BF_4)_4]^{8+}$, 588.59 $[M(BF_4)_3]^{9+}$, 521.03 $[M(BF_4)_2]^{10+}$, 465.76 $[M(BF_4)_1]^{11+}$. ESI-TOF-MS for **3** (positive mode): m/z = 1664.34 $[M(BF_4)_8]^{4+}$, 1314.07 $[M(BF_4)_7]^{5+}$, 1080.56 $[M(BF_4)_6]^{6+}$, 913.77 $[M(BF_4)_5]^{7+}$, 788.67 $[M(BF_4)_4]^{8+}$, 691.37 $[M(BF_4)_3]^{9+}$, 613.53 $[M(BF_4)_2]^{10+}$.

$[Co_6(R\text{-bisterpy})_6](C_{12}\text{-Glu})_{12}$ R = H (4), $OC_{16}H_{33}$ (5), $OC_{27}H_{55}$ (6). $[Co_6(R\text{-bisterpy})_6](BF_4)_{12}$ (0.01 mmol) in CH_3CN (20 mL) and $C_{12}\text{-Glu}^-Na^+$ (82.7 mg, 0.12 mmol) in MeOH (10 mL) were mixed and stirred for 3 h. Each product was obtained as an orange powder which was washed with acetonitrile. Yield of **4**: 39.4 mg (34%). Yield of **5**: 40.4 mg (31%). Yield of **6**: 41.9 mg (30%). Anal. $C_{648}H_{864}Co_6N_{48}O_{96}S_{12}$ (**4**): calcd. C 67.09, H 7.51, N 5.80; found. C 66.99, H 7.95, N 5.80. Anal. $C_{744}H_{1056}Co_6N_{48}O_{102}S_{12}$ (**5**): calcd. C 68.51, H 8.16, N 5.15; found. C 68.19, H 8.53, N 5.04. Anal. $C_{810}H_{1188}Co_6N_{48}O_{102}S_{12}$ (**6**): calcd. C 69.65, H 8.57, N 4.81; found. C 69.78, H 8.53, N 4.70.

Physical measurements

^1H NMR spectra were recorded on a JEOL (500-ECX) instrument (500 MHz) in deuterated solvents using TMS as internal reference. Elemental analyses (CHN) were carried out on a J-SCIENCE LAB JM10 analyser at the Instrumental Analysis Centre of Kumamoto University. ESI-TOF-MS measurements were measured on Xevo G2-XS QTof. TEM textures were collected on JEOL JEM-2100PLUS with accelerating voltage of 200 kV. Preparation of each sample involved adding one drop of its dichloromethane (or acetonitrile) solution (0.5 mM) on a carbon-coated Cu grid (Grid pitch 100 μm). DLS measurements were performed using a DLS-8000HL with a He-Ne laser. The concentration of DLS sample was adjusted to 0.5 mM. SAXS measurements was carried out using BL40B2 of SPring-8, Japan. The data were recorded using a Pilatus detector. The exposure time, the wavelength, and the sample-to-detector distance were 30 s, 0.15 nm, and 40 cm, respectively. Temperature-dependent magnetic susceptibilities were measured on a Superconducting Quantum Interference Device (SQUID) magnetometer at field strengths of 1 T with a sweep mode of 5 K min^{-1} in the temperature range of 5 to 400 K.

Fitting analysis of SAXS profiles

SAXS profiles of **4** and **5** were fitted by assuming the following relationship:

$$I(q) = x_1 P_{cyl}(q) S_{hex}(q) + x_2 P_{plate}(q) S_{lamellar}(q) \quad (1)$$

Here, x_1 and x_2 are the relative composition ratios of the hexagonal packed cylinder and the lamellar structure. $P_{cyl}(q)$ indicates the form factor of the core-shell cylinder with unlimited length given by

$$P_{Cyl}(q) \propto \frac{1}{q} \sum_{i=1}^{2} \left[\frac{V_i(\rho_i - \rho_{i+1}) F_1(qr_i)}{qr_i} \right]^2 \quad (2)$$

Here, F_1 represents the first-order Bessel function. ρ_i, V_i, and r_i represent the electron density of the i-th layer, the volume of the i-th layer, and the radius of the i-th layer, respectively. In Eq. (1), ρ_3 indicates the electron density of the space between cylinders.

The electron density of the space between cylinders, core, and shell were calculated from the following equation:

$$\rho = d \sum_i \rho_{w,i} w_i \quad (3)$$

Here, d represents the density of the mixed solvent, and $\rho_{w,i}$ and w_i represent the electron density per weight and the weight fraction for the i component, respectively. We also assumed the radius possessed a Gaussian distribution.

In table S1-3, the radius of the core and width of the shell represents r_c ($r_c = r_1$) and r_s ($r_2 = r_c + r_s$), respectively.

$P_{plate}(q)$ indicates the form factor of a plate with thickness La and unlimited expanse given by

$$P_{lamellar}(q) \propto \frac{\sin(\frac{qLa}{2})}{qLa/2} \quad (4)$$

The predicted thickness in our system may be less than 1 nm, but $P_{plate}(q)$ did not affect the shape of the fitting curve in La < 1 nm in the q range in Figure.3. Therefore, we could not determine the thickness of the plate.

$S_{hex}(q)$ and $S_{lamellar}(q)$ indicate the hexagonal and lamellar structural factors, respectively. These structural factors that contain the lattice spacing *dis* and the paracrystalline distortion factor *g* were reported by Hashimoto *et al* and Shibayama *et al*.[3,4] The subscripts of *L* and *h* in table S1-2 represent lamellar and hexagonal, respectively.

In the fitting analysis of **4**, Eq. (1) could not reproduce the experimental data well in the range of small q due to the presence of the amorphous aggregates. So, we added the baseline from the amorphous aggregates to Eq. (1) for **4**.

The SAXS profile for **6** was fitted by assuming the following relationship:

$$I(q) = yP_{cyl}(q)S_{hex1}(q) + (1-y)P_{cyl}(q)S_{hex2}(q) \quad (5)$$

In this equation it is assumed that there are two types of hexagonal packed structures with different stack spacings while there is one form factor $P_{cyl}(q)$.

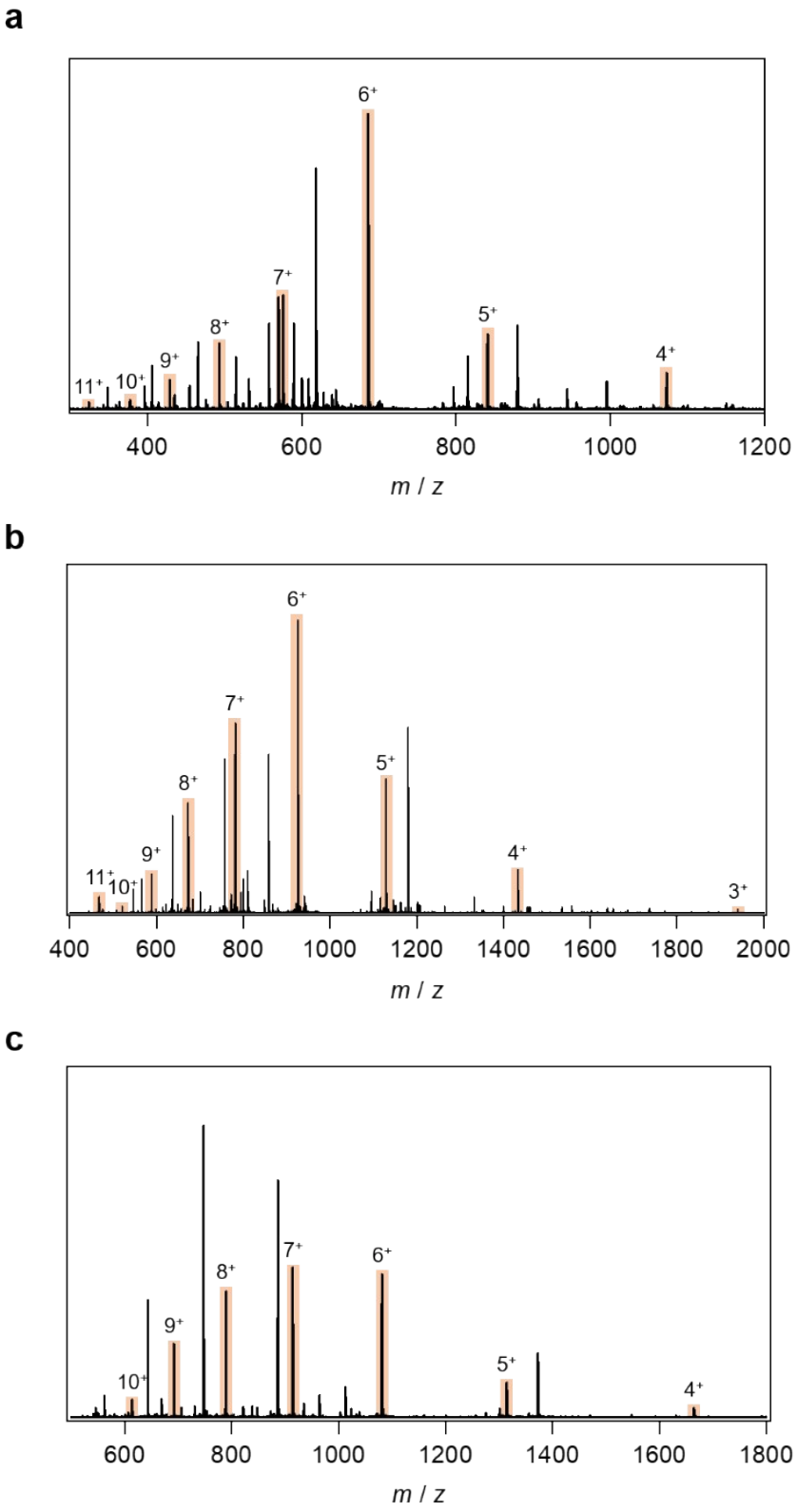

Fig. S1 ESI-TOF-MS spectra for **1**, **3** and **5** for positive mode in acetonitrile solution.

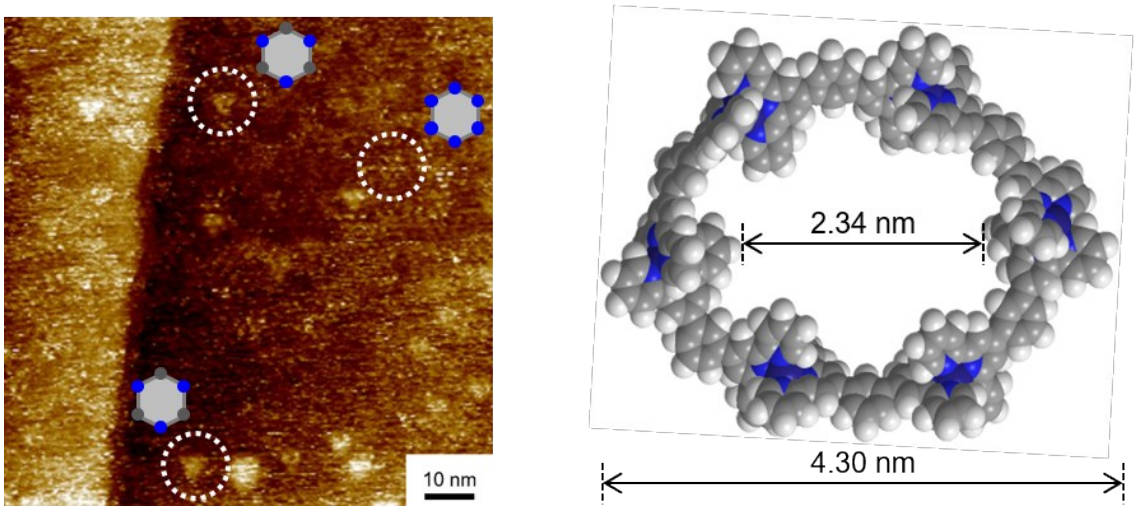

Fig. S2 STM texture for $[Co_6(bisterpy)_6](ClO_4)_{12}$ and CPK molecular model of $[Co_6(bisterpy)_6]^{12+}$.

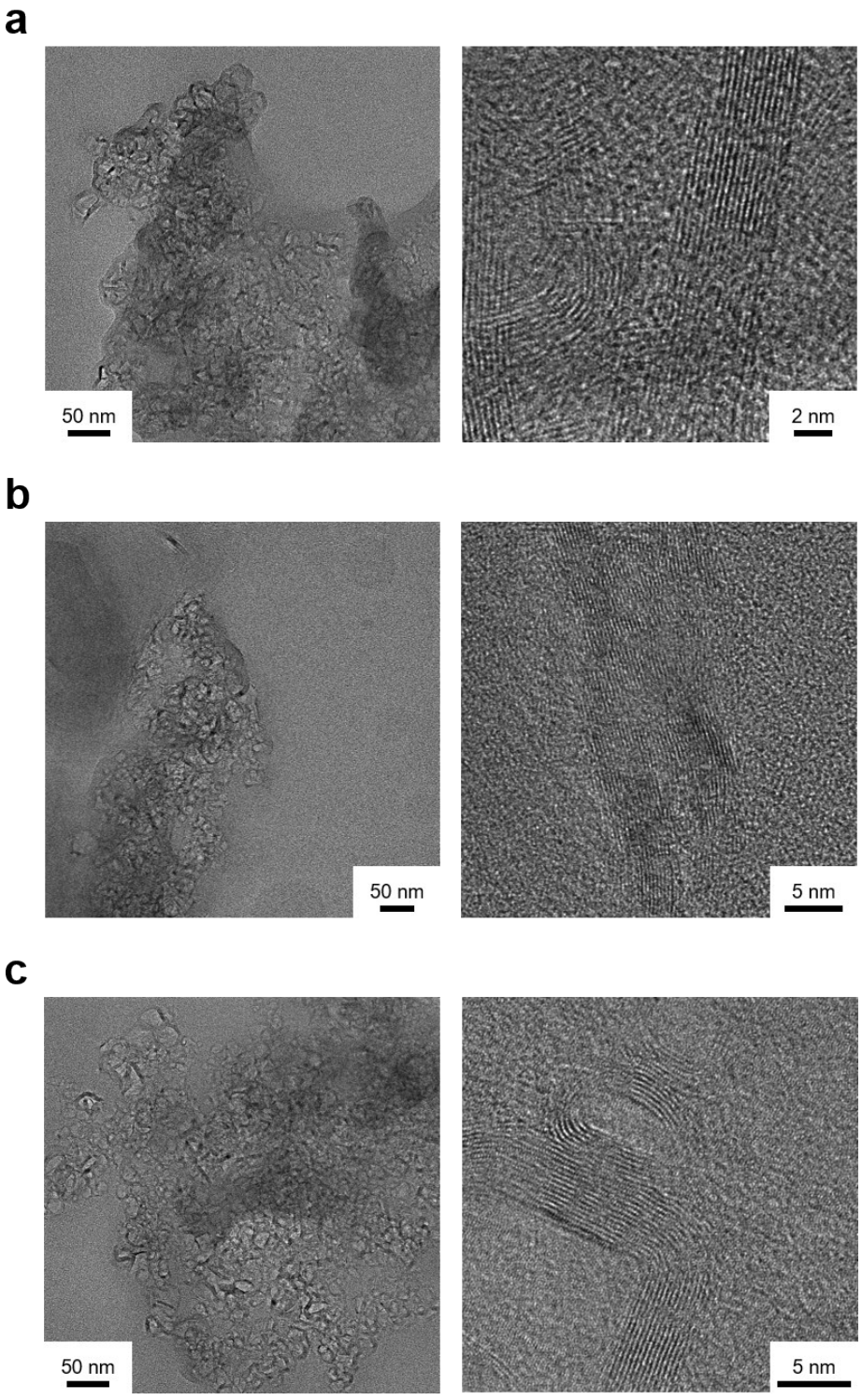

Fig. S3 TEM textures for **4**, **5** and **6** in dichloromethane solution.

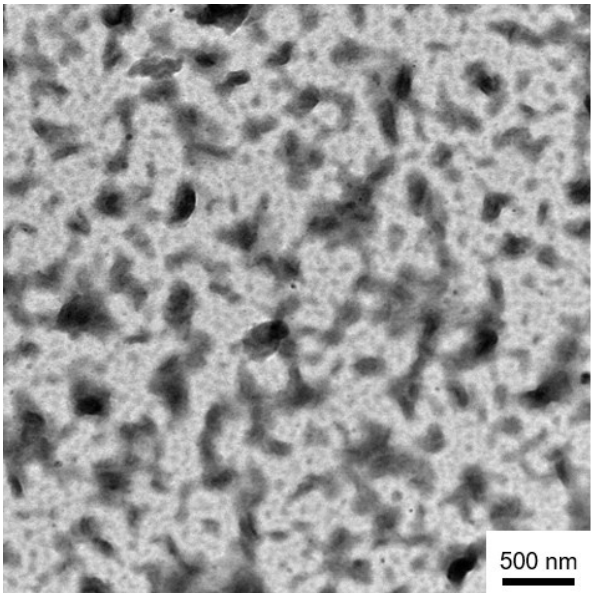

Fig. S4 TEM texture for **4** in ethanol solution.

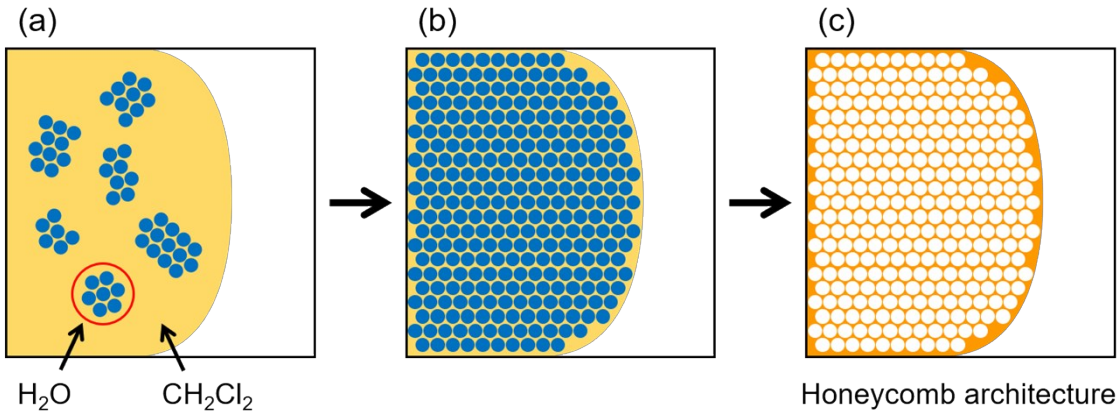

Fig. S5 Schematic illustration of the formation of a honeycomb architecture. (a) The solution surface temperature drops due to the evaporation of dichloromethane. Water micro-droplets condensed from atmospheric moisture are formed following evaporative cooling on the solution surface. (b) The water micro-droplets formed are transferred to the solution front by conventional flow or by capillary action. (c) After evaporation of the dichloromethane solution followed by the water micro-droplet, the honeycomb patterns are formed using a water droplet array as the template.

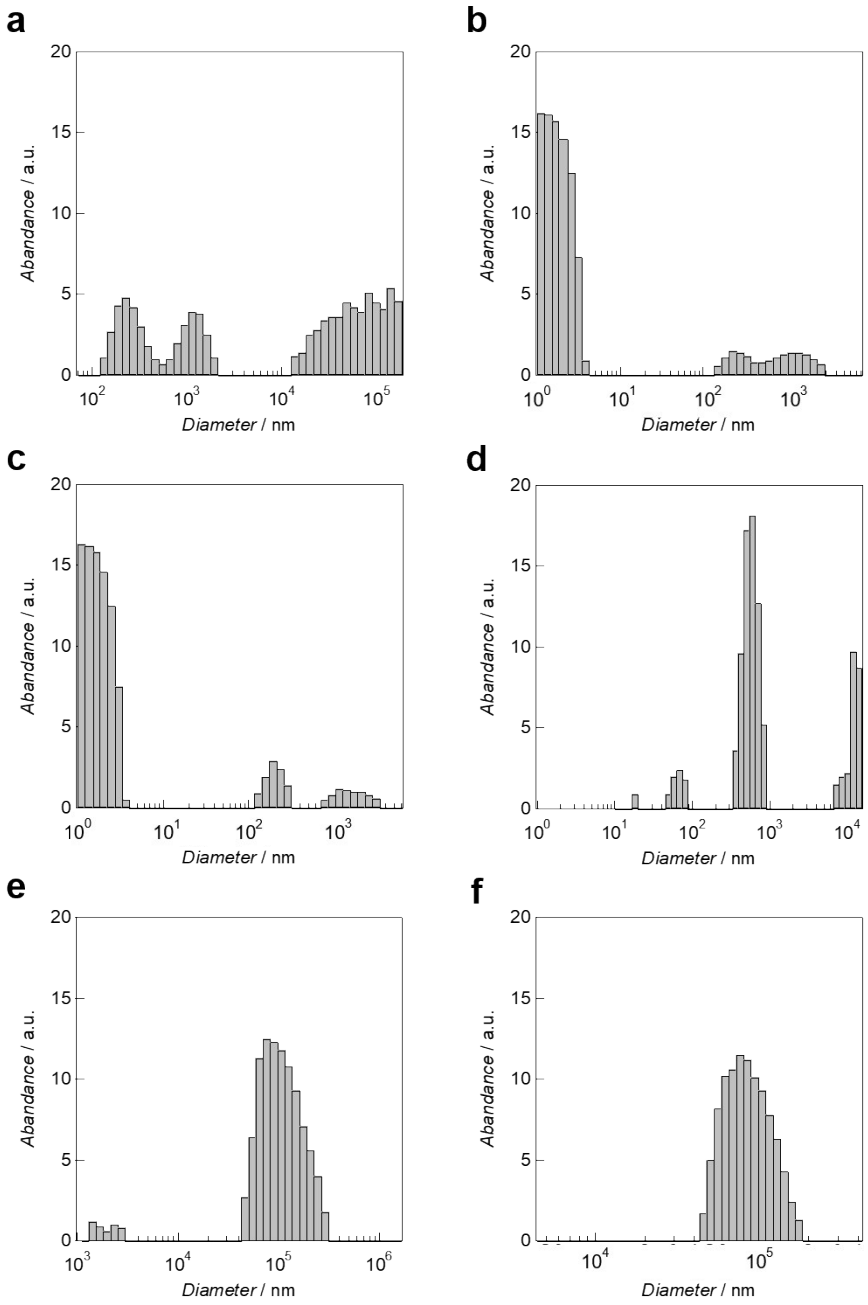

Fig. S6 Scattering intensity-based size distributions obtained by DLS analyses at 298 K. (a) **1**, (b) **2**, (c) **3** in acetonitrile. (d) **4**, (e) **5** and (f) **6** in dichloromethane.

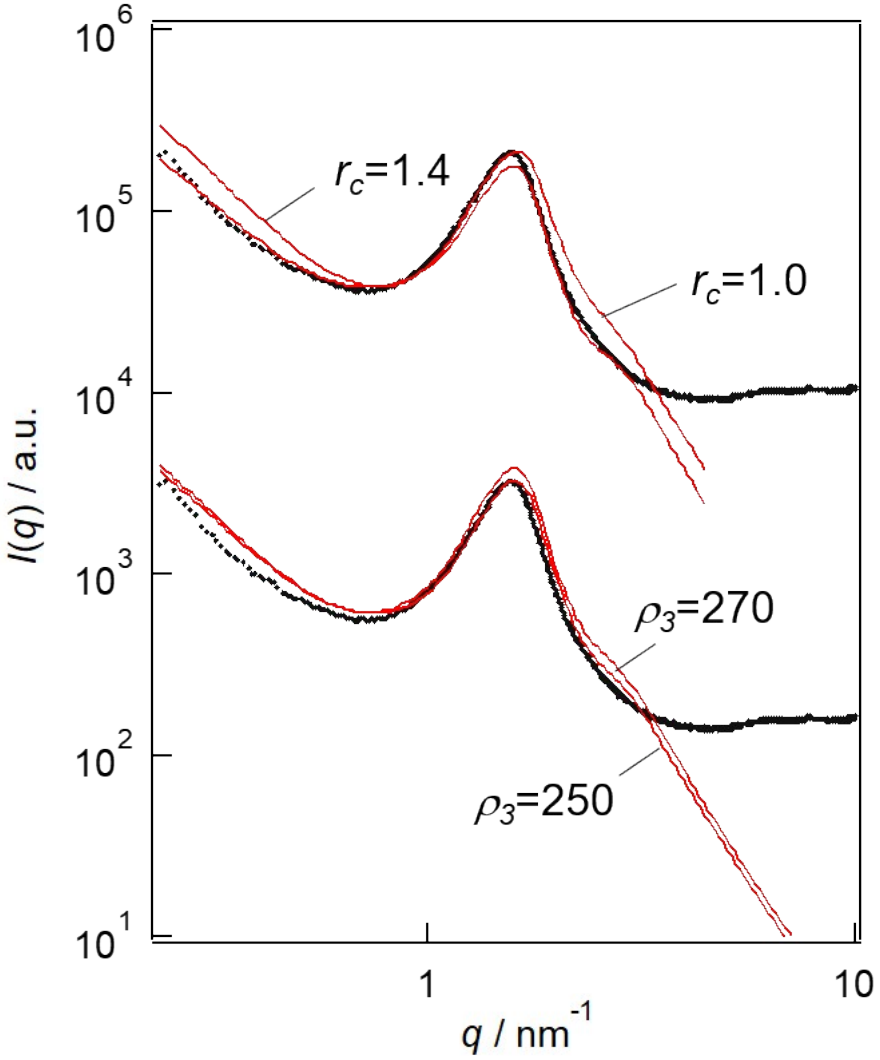

Fig. S7 Fitting of SAXS profiles for **4**. Theoretical curves (red) when one of the fitting parameters (r_c and ρ_3) was changed from the best fit combination with the experimental data (black).

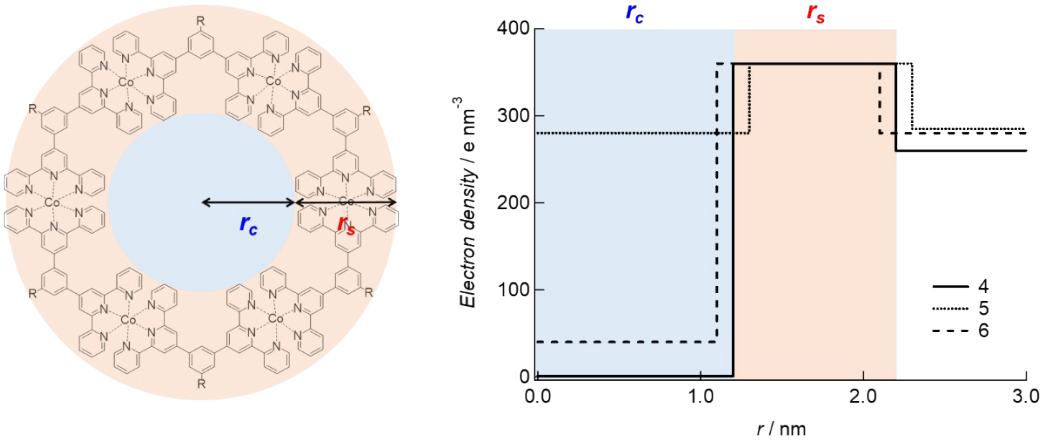

Fig. S8 Electron density for **4**, **5** and **6** obtained by fitting the SAXS profiles.

Table S1. SAXS fitting parameters for **4**.

$S_{lamellar}(q)$		$S_{hex}(q)$		$P_{cyl}(q)$					
dis_L (nm)	g_L	dis_h (nm)	g_h (nm)	r_c (nm)	r_s (nm)	ρ_1 (e/nm^3)	ρ_2 (e/nm^3)	ρ_3 (e/nm^3)	σ/r_c
4.3	0.25	3.65	0.175	1.2	1.0	1	360	260	0.33

Table S2. SAXS fitting parameters for **5**.

$S_{lamellar}(q)$		$S_{hex}(q)$		$P_{cyl}(q)$					
dis_L (nm)	g_L	dis_h (nm)	g_h	r_c (nm)	r_s (nm)	ρ_1 (e/nm^3)	ρ_2 (e/nm^3)	ρ_3 (e/nm^3)	σ/r_c
3.6	0.26	3.4	0.18	1.3	1.0	280	360	285	0.35

Table S3. SAXS fitting parameters for **6**.

$S_{hex1}(q)$		$S_{hex2}(q)$		$P_{cyl}(q)$					
dis_h (nm)	g_L	dis_h (nm)	g_h	r_c (nm)	r_s (nm)	ρ_1 (e/nm^3)	ρ_2 (e/nm^3)	ρ_3 (e/nm^3)	σ/r_c
3.4	0.18	3.5	0.08	1.1	1.0	40	360	280	0.36

$S_{hex}(q)$ and $S_{lamellar}(q)$ indicate the hexagonal and lamellar structural factors. $P_{cyl}(q)$ indicates the form factor of the core-shell cylinder.

References

1. P. Wang, C. N. Moorefield and G. R. Newkome, *Org. Lett.*, 2004, **6**, 1197.
2. R. Akiyoshi, K. Kuroiwa, S. Alao Amolegbe, M. Nakaya, R. Ohtani, M. Nakamura, L. F. Lindoy and S. Hayami, *Chem. Commun.*, 2017, **53**, 4685.
3. T. Hashimoto, T. Kawamura, M. Harada and H. Tanaka, *Macromolecules*, 1994, **27**, 3063.
4. M. Shibayama and T. Hashimoto, *Macromolecules*, 1986, **19**, 740.